Superdirective Broadside-Radiating Unidirectional Mixed-Multipole Antenna Arrays

Richard W. Ziolkowski
Department of Electrical and Computer Engineering, University of Arizona, Tucson, AZ, USA, ziolkows@arizona.edu

***Abstract*—A realistic superdirective broadside-radiating unidirectional mixed-multipole antenna (UMMA) design is presented and then used as the radiators of two two-element arrays. The single and two element systems are self-resonant in the 5G 28 GHz band being matched to 75 Ω sources without any intervening matching networks. Details of the designs along with their key performance attributes: directivity, realized gain, front-to-back ratio, radiation efficiency, and bandwidth, are given. It is demonstrated that these systems are not only highly efficient and have usable bandwidths, but they are all superdirective with their directivities surpassing several recognized bounds. They also further the recognition that traditional perceptions of superdirective systems being impractical are no longer tenable.**

***Index Terms*—Antenna theory, arrays, broadside-radiating, Huygens dipole antennas, multipoles, superdirectivity.**

I. Introduction

Compact antennas and arrays are at the research forefront because they will enable various promised traits of NextG wireless systems and their applications. The desires to overcome propagation losses, to have secure channels of information exchange, and to achieve efficient wireless power transfer have stimulated many investigations of highly directive systems. Superdirective radiating elements and/or arrays of them would facilitate those objectives.

The maximum directivity of a conventional broadside-radiating array/aperture antenna with transverse area, A, that is uniformly excited by a source whose wavelength is λ_0, is well-known. It is [1]: $D_{\max} = 4\pi\ A/\lambda_0^2$. Recall that gain is the product of efficiency times directivity and realized gain further accounts for any mismatch to the source. Consequently, $D_{\max}$ also represents their upper bounds. Any radiating system whose maximum directivity is larger than $D_{\max}$ is then said to be *superdirective* [1], [2].

There has been continuing engineering and physics interest in superdirective systems since the original needle radiation concept was introduced over 100 years ago [3]. The consensus opinion, which evolved in the last century, has been that superdirectivity is impractical because of very critical tolerances in fabrication and components, very low efficiencies, and extremely narrow bandwidths (e.g., [4], [5]). However, there have been several successful demonstrations of superdirective antennas and arrays, e.g., [6], [7], in the last two decades.

A recent approach to superdirectivity that is based on a mixture of multipoles [8] takes advantage of the well-known directivity limit established by Harrington [9], i.e., $D_{\max,\text{multipole}} = N^2 + 2N$ where N is the highest multipole order of an electric-magnetic antenna system. It has been shown theoretically that unidirectional needle-shaped patterns are obtainable even from an electrically small system by taking advantage of Huygens multipoles with high values of N [10]. End-fire and broadside radiating Huygens dipole antennas that are a mixture of electric and magnetic elements have reached the bound (mixture of electric and magnetic dipoles, giving $N = 1$, which leads to $D_{\max,\text{dipole}}$ = 3 = 4.77 dB) and have even slightly surpassed it in practice because of the presence of higher-order multipoles arising from their realistic, finite-size structures [11]. They are the simplest examples of the unidirectional mixed-multipole antenna (UMMA) concept.

A broadside-radiating, superdirective, electrically small UMMA that functions as a mixture of electric and magnetic dipoles and an electric quadrupole has been demonstrated [12], but its peak directivity was not close to the Harrington upper bound (i.e., with $N = 2$, $D_{\max,\text{quadrupole}}$ = 8 = 9.03 dB). On the other hand, several proof-of-concept broadside-radiating, superdirective UMMA designs based on mixtures of electric dipoles and quadrupoles were reported in [13] that surpass it. However, none of those designs were self-resonant; and, hence, they would require matching networks between them and a practical source. The associated losses would negatively impact their actual performance.

A self-resonant, superdirective, broadside-radiating UMMA matched to a 75 Ω source has been obtained with tailored modifications of one of those initial 28 GHz designs and is reported herein. Its design and performance characteristics are detailed in Sec. II. It is then used as the radiator in two two-element array configurations in Sec. III. These 28 GHz band arrays are self-resonant as well being matched by their designs to their 75 Ω sources. A brief summary of these self-resonant superdirective unidirectional systems is given in Sec. IV. All of these results were attained using the commercial software package AnsysEM21.1, i.e., the ANSYS high frequency structure simulator (HFSS), taking into account all realistic material properties (e.g., losses) and mutual coupling effects.

II. Broadside-radiating SR-UMMA Design

A 3D isometric view of the self-resonant UMMA design, SR-UMMA, is presented in Fig. 1. It is a stack of 3 Egyptian axe dipole (EAD) elements (metal layers) with two dielectric layers in between them. A top view of each EAD is given in Figs. 2(a)–(c). A side view of the stack is given in Fig. 2(d). The dielectric layers are rohacell ($\epsilon_r = 1.05$, loss tangent $= 4.0 \times 10^{-4}$), and the radius of the bottom and top rohacell layers are R_5 (bottom EAD radius) and R_3 (middle EAD

radius), respectively. The copper thickness of all of the EADs is 0.035 mm. This design was obtained by modifying the driven (top) EAD element of the UMMA-d2m system in [13]. The four short arms seen in Fig. 2(c) were added to it, and the design parameters were modified to engineer its input impedance to match the source impedance, 75 Ω. Notably, no detrimental consequences arose from the two adjacent to the feed lines, i.e., the currents on them were small and actually reinforced those on the striplines.

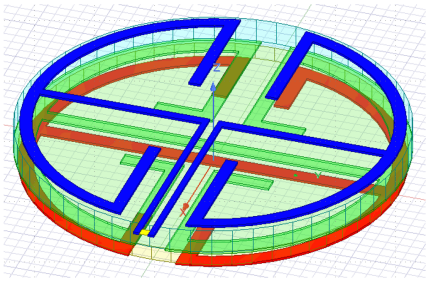

Fig. 1: Isometric view of the superdirective, broadside-radiating (peak in the +z-direction) 28 GHz SR-UMMA design. It consists of 3 metal and two rohacell layers. The source (yellow) is centered at the end of the striplines feeding the top EAD element.

The design parameters of each of its metal layers and the thicknesses of both rohacell disks are labeled and their optimized values are stated in millimeters. Including the copper layers, the total thickness is 0.07 $\lambda_{28\text{GHz}}$ = $\lambda_{28\text{GHz}}$ / 14.18, which is low-profile. The SR-UMMA design radiates fields in the broadside direction that are linearly polarized along the center trace direction of the EADs (i.e., along the y-axis).

The simulated $|S_{11}|$ values as a function of the source frequency are given in Fig. 3(a). It is clearly seen that the design is well matched to the 75 Ω source without any external matching elements, i.e., it is indeed self-resonant at 28.012 GHz where $|S_{11}|_{\text{min}}$ = –27.01 dB. The –10 dB and –6 dB bandwidths are 1.09 and 2.96, respectively, giving the fractional bandwidths with respect to 28.012 GHz: $FBW_{-10\text{dB}}$ = 3.89% and $FBW_{-6\text{dB}}$ = 10.57%. In fact, the –3 dB bandwidth is from 26.78 to 30.67 GHz giving $FBW_{-3\text{dB}}$ = 13.89%. The corresponding simulated front-to-back ratio (FTBR), peak directivity, and radiation efficiency (RE) values as functions of the source frequency are presented in Figs. 3(b)–(d), respectively. The green markers on the frequency (horizontal) axes denote the endpoints of the –10 dB impedance bandwidth.

The peak FTBR value, 32.47 dB, occurs at 27.975 GHz (λ_{ftbr} = 10.72 mm) with the RE = 96.2%. The maximum directivity at this frequency is 9.44 dB along the +z-axis with its backlobe level being –23.03 dB. The corresponding gain and realized gain values are, respectively, 9.26 and 9.25 dB, and the directivity patterns in its two principal planes are shown in Fig. 4(a). The unidirectional nature of this SR-UMMA design is immediately recognized. The slight asymmetry in the $\phi = 0°$ plane is due to the presence of the feedline strips. As illustrated in Fig. 3(b), the FTBR values are above 20.0 dB (14.9 dB) over the entire –10 dB (–6 dB) impedance bandwidth.

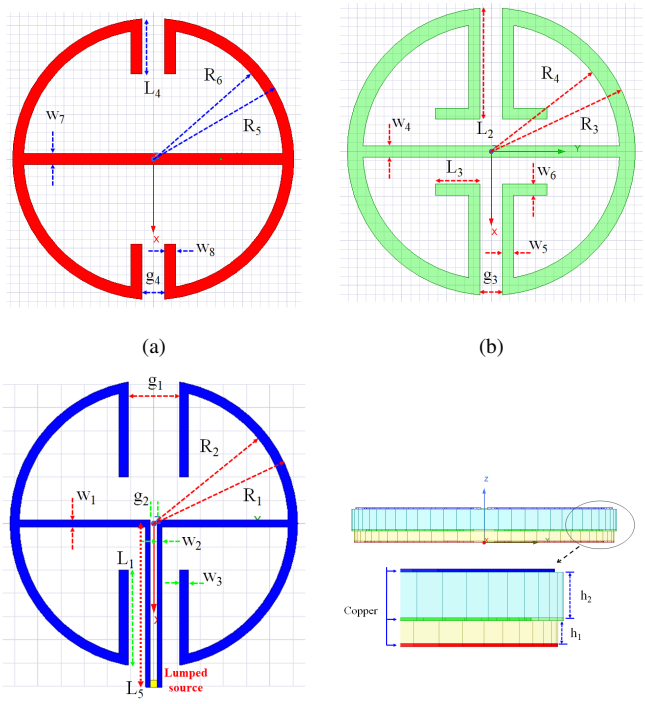

Fig. 2: The metal and rohacell layers of the 28 GHz SR-UMMA design matched to a 75 Ω source. All indicated dimensions are in millimeters.
(a) Bottom EAD: $g_4 = 0.50, w_7 = w_8 = 0.25, L_4 = 1.25, R_5 = 3.095, R_6 = 2.845, R_5 - R_6 = 0.25$;
(b) Middle EAD: $g_3 = 0.60, w_4 = w_5 = w_6 = 0.25, L_2 = 2.6, L_3 = 1.0, R_3 = 3.165, R_4 = 2.815, R_3 - R_4 = 0.35$;
(c) Driven, top EAD: $g_1 = 0.70, g_2 = 0.15, w_1 = 0.15, w_2 = 0.10, w_3 = 0.20, L_1 = 1.7, L_5 = 3.4815, R_1 = 3.065, R_2 = 2.865, R_1 - R_2 = 0.20$; and
(d) Side view: The thicknesses of the bottom and top rohacell layers are h_1 = 0.25 and h_2 = 0.40, respectively. Each EAD element is 0.035 mm thick (1 oz copper).

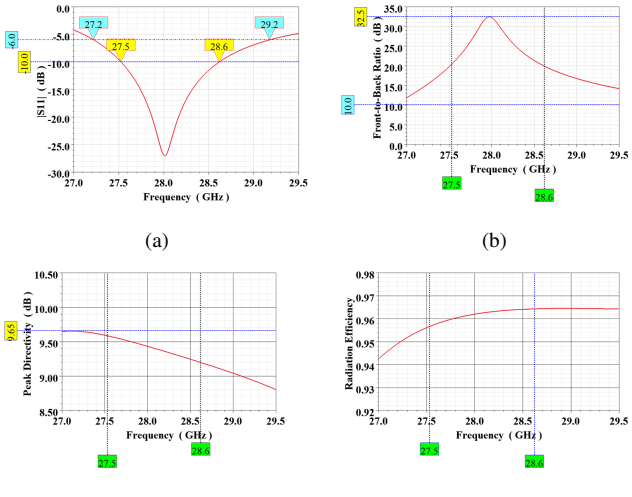

Fig. 3: Simulated performance characteristics of the 28 GHz SR-UMMA design as functions of the source frequency. (a) $|S_{11}|$ values. (b) FTBR values. (c) Peak directivity values. (d) RE values.

The peak directivity, 9.65 dB, occurs along the +z-axis at 27.10 GHz (λ_{dir} = 11.06 mm) with the RE = 94.6%. The corresponding gain value is 9.40 dB. The directivity patterns in the two principal planes at this frequency are shown in Fig. 4(b). With its backlobe level being -3.56 dB, the FTBR value at this frequency is 13.21 dB. As can be seen from Fig. 3(c), the maximum directivity is above 9.20 (8.96) dB over the entire –10 (–6) dB impedance bandwidth.

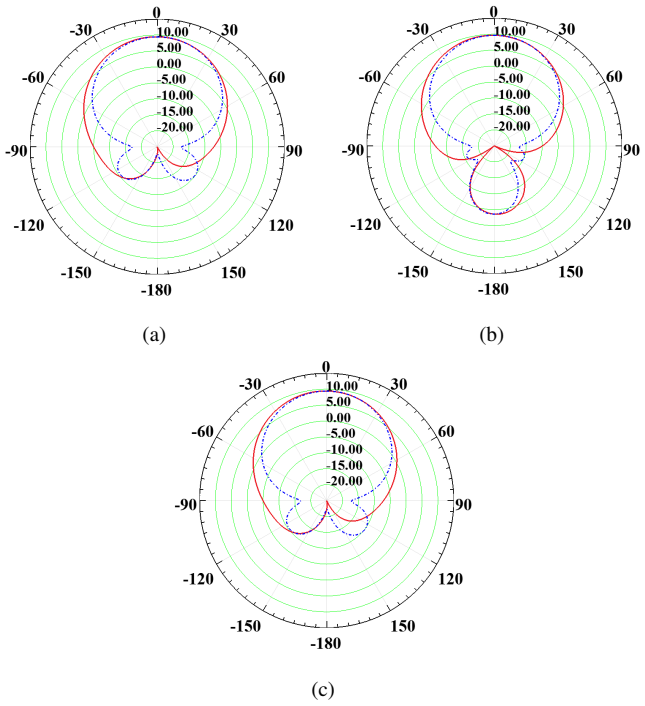

Fig. 4: Directivity patterns of the SR-UMMA design in its two principal planes: $\phi = 0°$ (red solid curve) and $\phi = 90°$ (blue dashed curve), at (a) 27.975 GHz (peak FTBR), (b) 27.10 GHz (peak directivity), and (c) 28.012 GHz (resonance).

The maximum directivity, gain, and realized gain and the FTBR and RE values at the resonance frequency, 28.012 GHz, are, respectively, 9.43 dB, 9.25 dB, 9.24 dB, 32.08 dB, and 96.2%. The corresponding directivity patterns are shown in Fig. 4(c). The differences in comparison to the peak FTBR patterns at that nearby frequency are quite small. These results effectively illustrate the robustness of the design in the neighborhood of the resonance frequency.

The 3-dB beamwidth at 27.10, 27.975, and 28.012 GHz in the $\phi = 0°$ plane is, respectively, 70.01°, 69.22°, and 69.23° – less than a 0.75% variation. Similarly, it is, respectively, 62.81°, 61.42°, and 61.40° in the $\phi = 90°$ plane – less than a 1.51% variation. The corresponding sidelobe level in the $\phi = 90°$ plane is, respectively, 24.55, 19.54, and 19.34 dB below the peak directivity.

The electrical size of the design at each of the frequencies of interest: 27.10, 27.975, and 28.012 GHz, is, respectively, ka = 1.798, 1.856, and 1.858. The aperture-size directivity bound for its circular aperture is $D_{\max} = 4\pi\,(\pi a^2)/\lambda_0^2 = (ka)^2$. Thus, with $a = R_3$ = 3.165 mm, $D_{\max}$ at the peak directivity, peak FTBR, and resonance frequencies is, respectively, 5.09 dB (3.23), 5.37 dB (3.44), and 5.38 dB (3.45). Consequently, with its directivities at these frequencies being above 9.4 dB, this 75 Ω SR-UMMA design is clearly superdirective. In particular, its maximum directivity, for example, at its resonance frequency exceeds that bound by 4.05 dB. It also surpasses the Harrington bound (8 or 9.03 dB for this dipole-quadrupole system with $N = 2$) by 0.40 dB, and the heuristic Kildal-Best upper bound [14]: ($D_{\mathrm{KB}} = ka^2 + 3$ = 1.858^2+3 = 6.45 = 8.10 dB) by 1.33 dB. It clearly exceeds these bounds at each of the other frequencies of interest.

Similar to the non-resonant version in [13], the RE values are exceptionally high, being nearly constant ($> 95.6\%$ with $< 0.84\%$ variation) over the entire –10 dB impedance bandwidth. They are also very high ($> 94\%$) across the entire –6 dB bandwidth. The difference in the peak directivity at 27.10 GHz and the maximum directivity at, for instance, 27.975 GHz is only 0.21 dB. These key frequencies are only 3.13% apart. In fact, the maximum directivity values are large ($>$ 8.96 dB) over the entire –6 dB impedance bandwidth. Note that the large contrast in the maximum FTBR values at these key frequencies arises simply because the SR-UMMA design reaches an exceptionally high peak value. Nevertheless, the SR-UMMA system is unidirectional (FTBR $\geq$ 10 dB) across its entire –6 dB bandwidth (and, in fact, over its entire –3 dB bandwidth).

As a comparison, the FTBR-constrained Rayleigh-Quotient (RQ) technique developed in [13] was applied to a 3-element linear array of ideal electric dipoles whose lengths and separations correspond to those of the center traces of the EADs in the SR-UMMA design. The dipoles were assumed to be z-oriented with the middle one on the z-axis. Their locations along the x-axis and lengths centered with respect to it were (in millimeters): d_1 = –0.25, d_2 = 0, d_3 = +0.40, L_1 = 6.13, L_2 = 6.33, and L_3 = 6.19. The FTBR constraint was set to –100 dB. Keeping all 16 digits of the solution coefficients, the directivity patterns at 28.0 GHz have a maximum directivity of 9.85 dB with a –90.15 dB backlobe, yielding FTBR = 100 dB. The SR-UMMA's maximum directivity is below this value by only 2.0%. However, keeping only 4 digits of the solution coefficients (which is a better numerical resolution than that yielded by the HFSS mixed-order solution with 227360 tetrahedra and a Delta S = 0.007), the maximum directivity and corresponding FTBR value reduce dramatically to 1.76 dB and 0.0 dB, respectively. The RQ-optimized result is highly sensitive to variations in the solution coefficients it generates. In fact, the highly-optimized RQ results degrade immediately away from the frequency at which the amplitude coefficients are obtained. In sharp contrast, the SR-UMMA's performance characteristics exhibit much less sensitivity across its entire operational bandwidth.

III. Broadside-Radiating Two-Element SR-UMMA Arrays

Two two-element arrays with the SR-UMMA as their radiators were considered. Both are broadside-radiating with their maximum directivities occurring along the +z-axis. The first

(single source case) is shown in Fig. 5(a); it follows from the array considered in [13]. Both elements share a single 75 Ω source as indicated. The distance between the centers of its two SR-UMMAs is 10.0 mm along the x-axis and, hence, their edges are separated by 3.67 mm ($\lambda/3.0$ at 27.0 GHz). The length of the strip feedlines of each SR-UMMA were simply extended by 1.5185 mm to achieve that center-to-center separation. The second (independent sources case) is shown in Fig. 5(b). Both elements are independently driven with 75 Ω sources as indicated. The distance between the centers of its two SR-UMMAs is 8.0 mm along the x-axis and, hence, their edges are separated by only 1.67 mm ($\lambda/6.4$ at 28.0 GHz). These SR-UMMAs were not modified in any manner. As will be demonstrated, this array configuration facilitates beam steering.

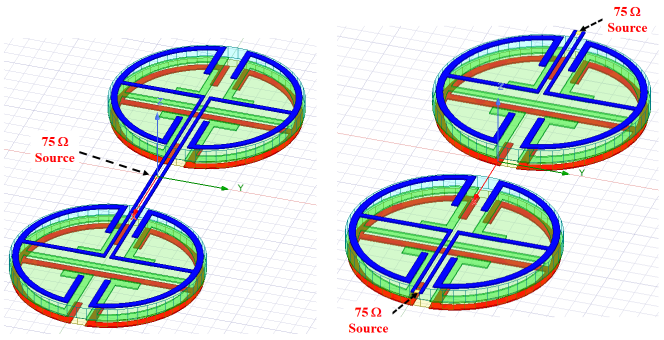

(a) (b)

Fig. 5: Isometric views of the superdirective, broadside-radiating, 28 GHz arrays formed with two SR-UMMAs. (a) Single source between the elements. (b) Two independent sources.

The simulated $|S_{11}|$ values as a function of the source frequency for the single source case are shown in Fig. 6(a). The presence of the second SR-UMMA, which loads the first one, has clearly impacted the overall resonance frequency, lowering it to 27.0 MHz where $|S_{11}|_{\min} = -17.40$ dB. The –10 dB and –6 dB bandwidths with respect to 27.0 GHz are 0.78 and 1.57 GHz, respectively, giving the fractional bandwidths $FBW_{-10\text{dB}} = 2.89\%$ and $FBW_{-6\text{dB}} = 5.81\%$. The peak directivity, 12.59 dB, occurs at 27.20 GHz. The FTBR value at this frequency is 16.50 dB and the radiation efficiency is 94.2%. The peak FTBR value, 32.95 dB, occurs at 27.80 GHz. The maximum directivity at this frequency is 12.49 dB and the radiation efficiency is 95.2%.

The maximum directivity, realized gain, FTBR, and radiation efficiency values at 27.0 GHz are 12.57 dB, 12.20 dB, 13.42 dB, and 93.6%, respectively. The corresponding unidirectional directivity patterns in the two principal planes of the array, i.e., $\phi = 0°$ and $\phi = 90°$, are displayed in Fig. 7(a). The small variation of the maximum directivity near the resonance frequency follows from the SR-UMMA's similar behavior. The beamwidth at 27.0 GHz in the $\phi = 0°$ plane is 29.00°; it is 59.81° in the $\phi = 90°$ plane. The difference in the beamwidths in these planes arises naturally from the fact that the array elements are located along the x-axis.

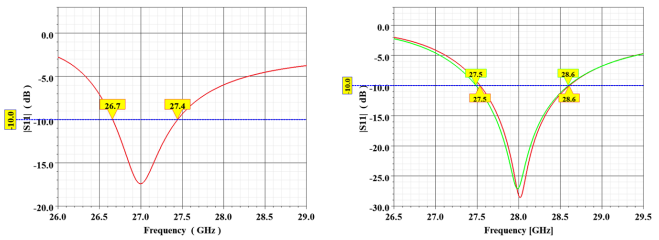

(a) (b)

Fig. 6: Simulated $|S_{11}|$ values as functions of the source frequency of the superdirective, broadside-radiating arrays formed with two SR-UMMAs. (a) Single source. (b) Two independent sources.

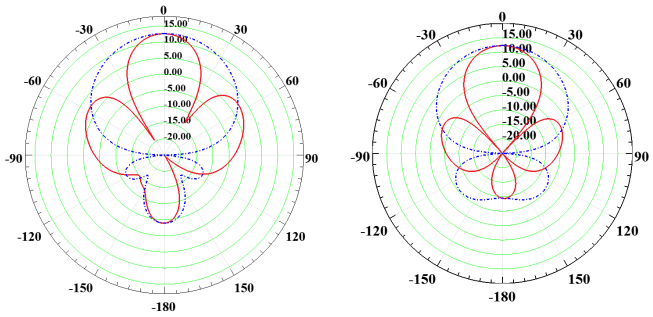

(a) (b)

Fig. 7: Directivity patterns at the resonance frequency in the two principal planes: $\phi = 0°$ (red solid curve) and $\phi = 90°$ (blue dashed curve) of the superdirective, broadside-radiating arrays formed with two SR-UMMAs. (a) Single source, 27.0 GHz. (b) Two independent sources, 28.0 GHz.

The simulated $|S_{11}|$ values as a function of the source frequency for the independent sources case are shown in Fig. 6(b). Despite the presence of the second SR-UMMA loading the first one and an even smaller separation distance, the resonance frequency of this two-element array is 28.02 GHz, where for both elements $|S_{11}|_{\min} < -27.0$ dB. This resonance frequency and the associated very good matches of each element to their sources' impedance at it are essentially the same as those of the SR-UMMA, i.e., the mutual coupling between the two elements of the array has little impact in this configuration. The –10 dB and –6 dB bandwidths are 1.07 and 1.92 GHz, respectively, giving the fractional bandwidths $FBW_{-10\text{dB}} = 3.81\%$ and $FBW_{-6\text{dB}} = 6.85\%$.

The peak directivity, 12.31 dB, occurs at 27.50 GHz. The FTBR value at this frequency is 20.90 dB and the radiation efficiency is 95.8%. The corresponding realized gain is 11.75 dB. The peak FTBR value, 23.14 dB, occurs at 27.75 GHz. The maximum directivity at this frequency is 12.30 dB and its radiation efficiency is 96.0%. The corresponding realized gain is 12.02 dB.

The maximum directivity, realized gain, FTBR, and radiation efficiency values at 28.0 GHz are 12.27 dB, 12.05 dB, 21.74 dB, and 96.2%, respectively. The corresponding unidirectional directivity patterns in the two principal planes of the array, i.e., $\phi = 0°$ and $\phi = 90°$, are displayed in Fig. 7(b). The beamwidth at 28.0 GHz in the $\phi = 0°$ plane is 34.21°; it

is 62.04° in the $\phi = 90°$ plane. Again, the difference in the beamwidths in these planes arises naturally from the fact that the array elements are situated along the x-axis.

The area in the xy-plane containing the single source (ss) and independent sources (is) arrays is, respectively, A_{ss} = 103.37 mm^2 and A_{is} = 94.72 mm^2. Thus, the upper bound on the maximum directivity at the resonance frequency of the single source and independent sources arrays is, respectively, $D_{\max,\mathrm{ss}} = 4\pi A_{ss}/\lambda^2_{27\mathrm{GHz}}$ = 10.54 = 10.23 dB and $D_{\max,\mathrm{is}} = 4\pi A_{is}/\lambda^2_{28\mathrm{GHz}} = 10.38$ = 10.16 dB. Consequently, since $D_{27\mathrm{GHz,ss}} = 12.57$ dB $> D_{\max,\mathrm{ss}}$ by 2.34 dB and $D_{28\mathrm{GHz,is}} = 12.27$ dB $> D_{\max,\mathrm{is}}$ by 2.11 dB, both arrays are demonstrated to be superdirective.

Note that the peak directivity of the independent sources case is slightly smaller than that of the single source case. This behavior occurs because the latter has a slightly larger aperture area. The beamwidths of the former are slightly larger for the same reason. Higher directivities and narrower patterns in the $\phi = 0°$ plane are expected if the linear array was composed of several more SR-UMMA elements. Similarly, the maximum directivity at the resonance frequency in the single source case is 3.14 larger than the SR-UMMA's value, while it is only 2.84 dB larger in the independent sources case. On the other hand, the overall bandwidth of the latter is larger and the variations of its performance characteristics over it are smaller than those of the former.

Successful beam steering is evidenced with the independent sources case. Given the center-to-center separation of its SR-UMMAs, a phase shift ± 0.4076 rad was applied to their sources to have the array's maximum directivity point at $\theta = +10°$ at 28.0 GHz. A small angle was elected as the example; more elements are needed to create a well-defined beam that effectively points to a much larger angle from broadside. The simulated directivity pattern in the two principal planes of the array at 28.0 GHz is displayed in Fig. 8. It is tilted in the $\phi = 0°$ plane as designed. The maximum directivity (realized gain), 12.07 (11.84) dB occurs at $\theta = +8°$. It is negligibly smaller, 12.01 (11.79) dB, at $\theta = +10°$. On the other hand, the shape of the directivity pattern in the $\phi = 90°$ plane does not change. Its maximum remains at $\theta = 0°$, but is reduced to 11.49 dB.

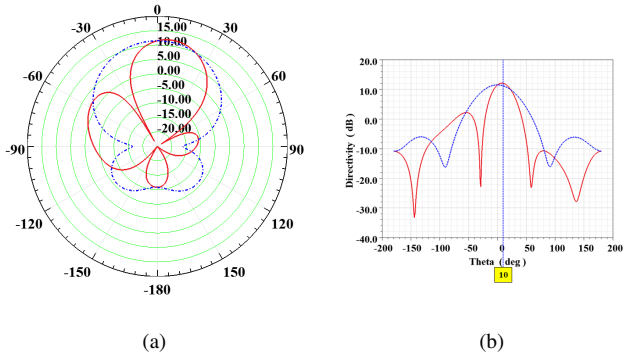

(a) (b)

Fig. 8: Directivity patterns in the two principal planes of the superdirective, broadside-radiating array formed with two independently addressable SR-UMMAs phased to point at $\theta = +10°$ at 28.0 GHz: $\phi = 0°$ (red solid curve) and $\phi = 90°$ (blue dashed curve). (a) Polar. (b) Linear.

IV. Conclusions

A 28 GHz SR-UMMA design that is matched to a 75 Ω source and its simulated performance characteristics were presented. It was demonstrated that this broadside-radiating SR-UMMA system is superdirective, has a very high radiation efficiency, and exhibits a very usable bandwidth. Its directivity was also shown to surpass several recognized (e.g., the Harrington and Kildal-Best) bounds. The SR-UMMA was then used to form two two-element arrays that were also matched to 75 Ω sources. One was excited by a single source shared by the two SR-UMMAs and was self-resonant at 27.0 GHz. Each SR-UMMA of the second array had its own source and was self-resonant at 28.0 GHz. Modest beam steering with proper phasing of those independent sources was also evidenced. The performance characteristics of each array were described. Both arrays were demonstrated to be superdirective. These broadside-radiating systems further manifest the robustness of the mixed-multipole paradigm for attaining practical, unidirectional antennas that have very attractive directivity properties. Their performance characteristics further refute the commonly held belief that practical superdirective systems are not achievable.

References

[1] C. A. Balanis, *Antenna Theory: Analysis and Design*, 4th ed. Hoboken, NJ, USA: John Wiley & Sons, 2016.

[2] R. C. Hansen, "Fundamental limitations in antennas," *Proc. IEEE*, vol. 69, no. 2, pp. 170–182, Feb. 1981.

[3] C. W. Oseen, "Die einsteinsche nadelstichstrahlung und die Maxwellschen gleichungen," *Ann. Phys.*, vol. 374, no. 19, pp. 202–204, 1922.

[4] R. C. Hansen, "Some new calculations on antenna superdirectivity," *Proc. IEEE*, vol. 69, no. 10, pp. 1365–1366, Oct. 1981.

[5] R. W. King, "Supergain antennas and the Yagi and circular arrays," *IEEE Trans. Antennas Propag.*, vol. 37, no. 2, pp. 178–186, Feb. 1989.

[6] A. D. Yaghjian, T. H. O'Donnell, E. E. Altshuler, and S. R. Best, "Electrically small supergain end-fire arrays," *Rad. Sci.*, vol. 43, no. 3, 2008.

[7] A. Clemente, M. Pigeon, L. Rudant, and C. Delaveaud, "Design of a super directive four-element compact antenna array using spherical wave expansion," *IEEE Trans. Antennas Propag.*, vol. 63, no. 11, pp. 4715–4722, Nov. 2015.

[8] R. W. Ziolkowski, "Mixtures of multipoles — Should they be in your EM toolbox?" *IEEE Open J. Antennas Propag.*, vol. 3, pp. 154–188, 2022.

[9] R. F. Harrington, "On the gain and beamwidth of directional antennas," *IRE Trans. Antennas Propag.*, vol. 6, no. 3, pp. 219–225, Jul. 1958.

[10] R. W. Ziolkowski, "Using Huygens multipole arrays to realize unidirectional needle-like radiation," *Phys. Rev. X*, vol. 7, no. 3, 031017, Jul. 2017.

[11] ——, "Electrically small antenna advances for current 5G and evolving 6G and beyond wireless systems," in *Antenna and Array Technologies for Future Wireless Ecosystems*, Y. J. Guo and R. W. Ziolkowski, Eds. Hoboken, NJ, USA: John Wiley & Sons, 2022, pp. 335–391.

[12] T. Shi, M.-C. Tang, R. Chai, and R. W. Ziolkowski, "Multipole-based electrically small unidirectional antenna with exceptionally high realized gain," *IEEE Trans. Antennas Propag.*, vol. 70, no. 7, pp. 5288–5301, Jul. 2022.

[13] R. W. Ziolkowski, "Superdirective unidirectional mixed-multipole antennas: Designs, analysis, and simulations," *IEEE Trans. Antenna Propag.*, vol. 71, no. 7, pp. 5566–5581, Jul. 2023.

[14] P.-S. Kildal and S. R. Best, "Further investigations of fundamental directivity limitations of small antennas with and without ground planes," in *Proc. 2008 IEEE Antennas and Propagation Society International Symposium*, San Diego, CA, 05–11 July 2008.